Research Article

Examination of Environmental Factors Influencing the Emission Rates of Semivolatile Organic Compounds

Sunwoo Lee[1] and Janghoo Seo [ID][2]

[1]Zero-Energy Appropriate Technology Institute, Seoul Energy Dream Center, 14 Jeungsan-ro, Mapo-gu, Seoul 03901, Republic of Korea
[2]School of Architecture, Kookmin University, 77 Jeongneung-ro, Seongbuk-gu, Seoul 02707, Republic of Korea

Correspondence should be addressed to Janghoo Seo; seojh@kookmin.ac.kr

Some types of semivolatile organic compounds (SVOCs) that are emitted from plastics used in building materials and household appliances have been associated with health risks, even at low concentrations. It has been reported that di-2-ethylhexyl phthalate (DEHP)—one of the most commonly used plasticizers—causes asthma and allergic symptoms in children at home. The amount of emitted DEHP, which is classified as a SVOC, can be measured using a microchamber by the thermal desorption test chamber method. To accurately measure the SVOC emission rates, the relation between SVOC and environmental factors should be clarified. Herein, we examined the effects of the temperature, relative humidity, concentration of airborne particles, and flow field in the microchamber on SVOC emission rates. The flow fields inside the microchamber were analyzed via computational fluid dynamics (CFD). The emission rate of SVOC released from PVC flooring increased under high temperatures and at high concentrations of airborne particles but did not depend on the relative humidity. From an evaluation performed using an index of air change efficiency, such as the air age and the coefficient of air change performance, we found that a fixed air exchange rate of $1.5\,h^{-1}$ in the microchamber is desirable.

1. Introduction

Semivolatile organic compounds (SVOCs) are used as plasticizers in building materials, interior materials, furniture, and consumer electronics. At home, these SVOCs mix with house dust. Therefore, there is a concern over the health effects of SVOCs because there is a risk that they may cause asthma and allergic symptoms in children at home [1–15].

The thermal desorption test chamber (TDC) method was developed in Japan. This technique can be employed to determine the emission rates of SVOCs under room-temperature conditions using a microchamber [16–19]. Additionally, a TDC-based microchamber method approach was standardized as JIS A 1904 as a method for determining the emission of SVOCs from building materials [20].

We verified the accuracy of the measurements using a microchamber and the TDC method as well as the reproducibility of the microchamber method. They determined the

emission rate of SVOCs from various types of materials and investigated the recovery ratios of the microchamber using reference materials [18, 21]. Next, they selected a number of factors, including background concentration, loading factor, specimen orientation, time, type of gas supplied, and process effects on the inner surface of the microchamber, which were expected to affect the emission behavior of SVOCs with the microchamber method and reported the results [21, 22]. Meanwhile, the temperature, relative humidity, air exchange rate, and other factors have been considered to affect the emission rate of chemicals using JIS A 1901 and other general test chamber methods [23]. Although it may be predicted that the aforementioned factors can also influence the measurement of SVOC emission rates using the microchamber method, there are a few investigated cases. Moreover, SVOCs have an extremely low volatility and are easily adsorbed to the surfaces of solids. To investigate the factors that influence the emission rate of SVOCs, it is essential to investigate the
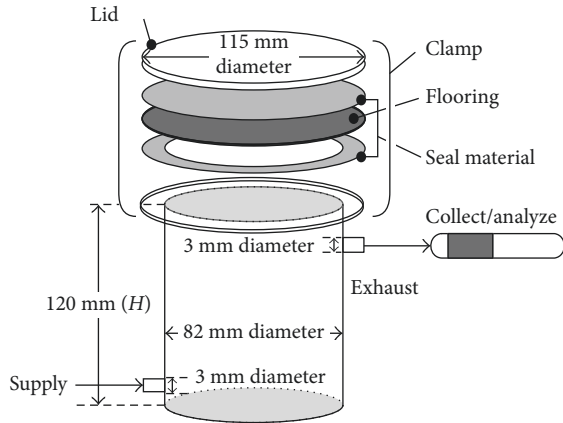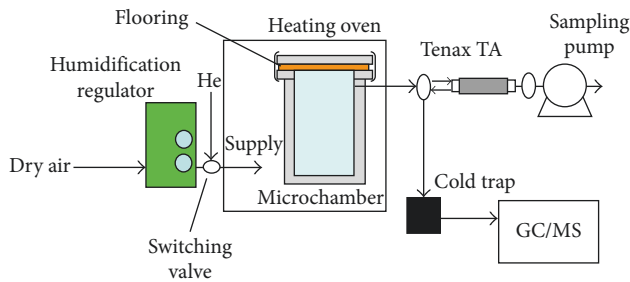
FIGURE 1: Schematic of the microchamber.

FIGURE 2: Schematic of the thermal desorption test chamber system.

correlation between the SVOC emission rate and airborne particles in the room. Herein, we study the dependence of the emission rate of di-2-ethylhexyl phthalate (DEHP)—an SVOC—on the temperature, relative humidity, and airborne particles. Additionally, we investigated the influence of varying the air exchange rate properties of the microchamber on its flow field using computational fluid dynamics (CFD).

2. Method

2.1. Microchamber System. Figure 1 shows a schematic of the microchamber, which is made of glass and has been treated with silane. The microchamber is cylindrical (82 mm (diameter) × 120 mm (height)). Air enters the microchamber through an inlet (inner diameter = 3 mm) at the lower side of the cylinder (13 mm from the bottom). Directly opposite to this inlet, on the upper side of the cylinder (96 mm from the bottom), there is a collection outlet (inner diameter = 3 mm). On top of the microchamber, there is a 15 mm rim on which a glass lid (diameter = 11.5 mm) is placed. A clamp is used to hold a seal and a flooring material in place while keeping the interior of the microchamber airtight. The emission area of the building material is 5.3×10^3 mm^2.

Figure 2 shows a schematic of the thermal desorption test chamber system. SVOCs are easily adsorbed by the microchamber walls under room-temperature conditions. The thermal desorption test chamber method measures emissions based on the adsorbed constituents. After collecting

TABLE 1: Measurement conditions of the thermal desorption test chamber system.

SVOC constituent adsorption process	
Gas supply	Air
Temperature and humidity	28°C and 50% RH
Air exchange rate	1.5 h^{-1}
Loading factor	8.4 m^2/m^3
Sampling rate	23 L (16 ml/min × 24 h)
Scavenger	Tenax TA (60/80)
SVOC constituent thermal desorption process	
Gas supply	Helium (90 ml/min)
Air exchange rate	4.6 h^{-1}
Sampling rate	75 min/3.75 L
Temperature of the thermal desorption system	28°C (30 min)→ 15°C/min→200°C (30 min)
Scavenger	Tenax TA (60/80)

TABLE 2: Analytical conditions of the gas chromatography/mass spectrometry thermal desorption system (GC/MS-TDS).

GC/MS	Agilent HP6890-G1530A/HP5973MSD
Column	TC5 0.25 μm × 0.25 mm (I.D.) × 30 m (GL science)
Oven temperature	40°C (2 min)→15°C/min→270°C (21 min)
Split ratio	50 : 1
CIS	−130°C (1.5 min)→12°C/min→300°C (10 min)
TDS	20°C (5 min)→60°C/min→280°C (10 min)

the gas emissions from the specimen under room-temperature conditions, the sample is removed from the microchamber and heated at a high temperature. The SVOC constituents adsorbed to the interior of the microchamber are collected, and the emission rate is determined by summing the two [16].

2.2. Recovery of the Microchamber. Assuming that the SVOCs emitted from the material will adsorb to the microchamber walls, the recovery rate was calculated using a reference standard SVOC substance. A predetermined amount of the reference SVOC material was directly added to Tenax TA. In total, 2 μL of the reference SVOC solution was injected into the microchamber using a syringe. Then, thermal desorption was performed immediately. From the amount of SVOC collected, it was confirmed that the recovery rate was at least 90%. Tables 1 and 2 list the measurement conditions of the thermal desorption test chamber system and the analytical conditions of the gas chromatography/ mass spectrometry thermal desorption system (GC/MS-TDS), respectively.

2.3. Measurements. Table 3 lists the test cases. In case 1, PVC flooring was used as the specimen (this flooring has been reported to emit DEHP, which is an SVOC). The flooring specimen was placed inside a desiccator and cured. After one day of curing, it was removed. The air supplied to the desiccator had a temperature of 28°C ± 1°C and a relative humidity (RH) of 50% ± 5%. PVC flooring was placed inside

TABLE 3: A list of test cases (air exchange rate = $1.5\,h^{-1}$).

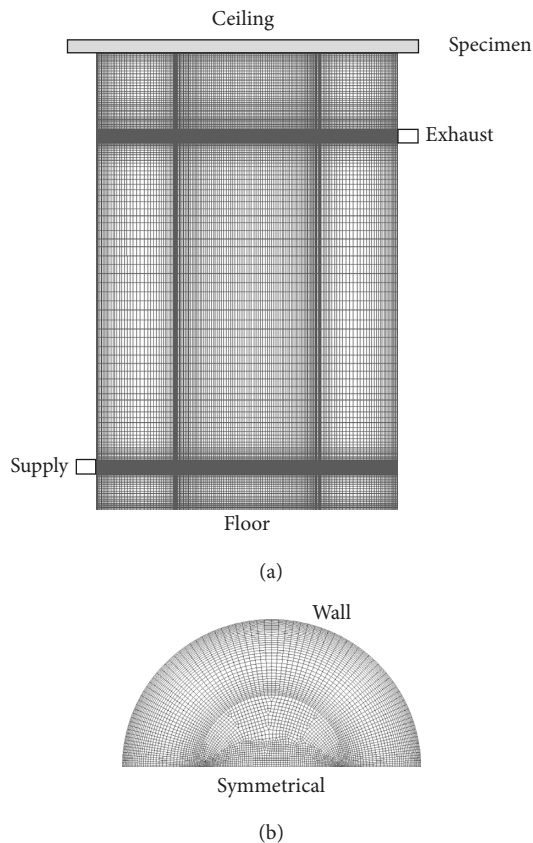| Case	Temperature (°C)	Relative humidity (%)	Airborne particles	SVOC adsorption area
1	28	50	—	Inner wall of the chamber
2	40	50	—	Inner wall of the chamber
3	28	40	—	Inner wall of the chamber
4	28	70	—	Inner wall of the chamber
5	28	50	Quartz wool: 170 mg	Inner wall of the chamber + quartz wool
6	28	50	Quartz wool: 340 mg	Inner wall of the chamber + quartz wool

(a)

(b)

FIGURE 3: Schematic of the analytical mesh: (a) vertical cross section (symmetrical) and (b) horizontal cross section.

the microchamber, and the test was conducted under the following conditions: temperature = 28°C, RH = 50%, and air exchange rate = $0.5\,h^{-1}$. The sample was a 115 mm diameter circle of flooring cut from the center of a roll of flooring (as shown in Figure 1, the emission area had a diameter of 82 mm due to the seal).

To ensure the reproducibility of the volume of chemicals emitted from the flooring specimen, the test performed in case 1 was repeated three times under the same conditions. The temperature inside the chamber was set to 28°C and 40°C, and the dependence of the SVOC emission rate on the temperature was investigated.

The temperature in the high-temperature condition was set to 40°C considering the rise in the surface temperature of building materials placed in a location with good exposure to sunlight and the rise in the temperature of the surface of

consumer electronics when running. The RH was set to 40, 50, and 70%, and the influence of the changes in the RH on the SVOC emission rate was confirmed. The RH was set to 40% and 70% because Japan's Act on Maintenance of Sanitation in Buildings sets the environmental standard for RH in offices between 40% and 70%. Additionally, quartz wool was placed inside the microchamber, and the authors investigated the influence of the changes in the adsorption area due to the presence or absence of airborne particles. This wool was heated and cleaned before the experiment. As with the measurement of the recovery rate in the microchamber, we calculated the DEHP collection rate in the microchamber for cleaned quartz wool and confirmed a recovery rate of at least 90%. To confirm that the SVOC emission rate was in a steady state, the emissions were sampled five times in case 1 (0.5, 3, 12, 24, and 48 h after the experiment began) and three times in case 2 (0.5, 3, and 24 h after the experiment began). In the other cases, the emissions were sampled 0.5 and 24 h after the experiment began, and the rate of SVOC emissions from the flooring specimen over time was investigated.

2.4. Numerical Method. Figure 3 shows a schematic of the analytical mesh. Tables 4 and 5 list the CFD analysis cases and conditions, respectively. The inlet boundary conditions were set as follows: air exchange rate = $1.5\,h^{-1}$ ($U_{in} = 2.1 \times 10^{-2}$ m/s), $0.8\,h^{-1}$ ($U_{in} = 3.9 \times 10^{-2}$ m/s), and $4.0\,h^{-1}$ ($U_{in} = 5.2 \times 10^{-2}$ m/s). Additionally, the air age and the coefficient of the air change performance η in the microchamber were investigated [23]. The air age is defined as the length of time t during which a specific amount of outdoor air has been in a building, zone, or space, and the coefficient of the air change performance is defined as an air distribution system's ability to deliver ventilation air to a building, zone, or space [24]. A three-dimensional analysis was performed based on a flow field of the low-Reynolds (Re)-type k–ε model (Abe–Nagano model) [25]. Given the symmetry of the interior of the microchamber, only half of the area was subjected to analysis.

After analyzing the flow field, the surface gas-phase concentration of DEHP was set in the specimen position and the diffusion field was analyzed. Table 5 lists the DEHP surface gas-phase concentration (C_0) and air diffusion coefficient (D_a) values [26, 27]. When determining the amount of DEHP emitted from the flooring specimen, it should be set as an internal diffusion-controlled building material; however, for computational convenience, this study's model is set as an evaporation-controlled building material. The concentration of the air flowing into the microchamber via

TABLE 4: A list of computational fluid dynamics (CFD) analysis cases (temperature = 28°C).

Case	Air exchange rate (h^{-1})	U_{in} (m/s)	Mass transfer coefficient* (m/h)
7	0.8	2.1×10^{-2}	0.9
8	1.5	3.9×10^{-2}	3.5
9	4.0	5.2×10^{-2}	7.7

*The mass transfer coefficients in cases 7–9 are converted to water vapor. These values are calculated via CFD analysis [20].

TABLE 5: A list of CFD analysis conditions.

Mesh divisions	Approximately 890,000
Turbulence model	Low-Reynolds (Re)-type k–ε model (Abe–Nagano model)
Difference scheme	First-order windward
Supply boundary	$U_{in} = 2.1 \times 10^{-2}$ m/s (case 7), 3.9×10^{-2} m/s (case 8), and 5.2×10^{-2} m/s (case 9) $L_{in} = 3.0 \times 10^{-3}$ m, $k = 3/2$ $(U_{in} \times 0.015)^2$, and $L = 1/7 \cdot L_{in}\varepsilon = C_u \cdot k^{3/2}/L$
Exhaust boundary	U_{out}: via mass conservation; k_{out}, ε_{out}: free slip
Wall surface boundary	No slip

DEHP surface gas-phase concentration at 28°C (C_s) = 298.3 μg/m^3; DEHP air diffusion coefficient at 28°C (D_a) = 7.1×10^{-7} m^2/s.

TABLE 6: Test results (air exchange rate = 1.5 h^{-1}).

Case	Temperature (°C)	Relative humidity (%)	Airborne particles	SVOC adsorption area	DEHP collection volume (ng) 0.5 h after the exp. began	24 h after the exp. began	DEHP emission rate (μg/m^{2}h) 0.5 h after the exp. began	24 h after the exp. began
1	28	50	—	Inner wall of the chamber	131.9	1686.4	49.8	13.3
2	40	50	—	Inner wall of the chamber	184.0	5365.0	69.4	42.2
3	28	40	—	Inner wall of the chamber	100.0	1293.6	37.7	10.2
4	28	70	—	Inner wall of the chamber	240.0	1172.5	90.6	9.2
5	28	50	Quartz wool: 170 mg	Inner wall of the chamber + quartz wool	335.9	2733.0	126.8	20.6
6	28	50	Quartz wool: 340 mg	Inner wall of the chamber + quartz wool	671.8	3723.0	253.5	29.1

the air inlet was set to zero, and the constant concentration was calculated under isothermal conditions (28°C).

3. Results

Table 6 and Figures 4–6 show the measurements of the rate at which DEHP was emitted from the flooring specimen due to influencing factors, including temperature, RH, and airborne particles.

3.1. Relation between the DEHP Emission Rate and Temperature. In case 1, 0.5 h after the initiation of the experiment, the rate at which DEHP was emitted from the flooring specimen was 49.8 μg/m^{2}h. However, over time, the DEHP emission rate decreased. Approximately 10 h after the initiation of the experiment, the DEHP emission rate reached a steady state. At this point, the DEHP emission rate was 13.3 μg/m^{2}h (Table 6 and Figure 4). In case 2, the temperature was set to 40°C considering the rise in the temperature of the surface of the flooring specimen because of the exposure to sunlight or the like. In this case, 24 h after the initiation of the

experiment, the rate at which DEHP was emitted from the flooring specimen was 42.2 μg/m^{2}h. As shown in Figure 4, we confirmed that the emission rate of DEHP was dependent on the temperature.

The DEHP emission rate determined 24 h after the initiation of the experiment is an average value over three measurements; the relative standard deviation (RSD) is 4%.

3.2. Relation between DEHP Emission Rate and RH. In case 3, the RH was set to 40%. 0.5 and 24 h after the start of the experiment, the rates of DEHP emissions from the flooring specimen were 37.7 and 10.2 μg/m^{2}h, respectively. Thus, the DEHP emission rates obtained in this case were not considerably different from those obtained in case 1 wherein the RH was set to 50%. Furthermore, in case 4, the relative humidity was set to 70%, and 24 h after the initiation of the experiment, the rate at which DEHP was emitted from the flooring specimen was 9.2 μg/m^2·h. Katsumata et al. reported that there were almost no differences in the DEHP emission rates, regardless of whether the air supplied to the microchamber was humidified or dry [16]. The present
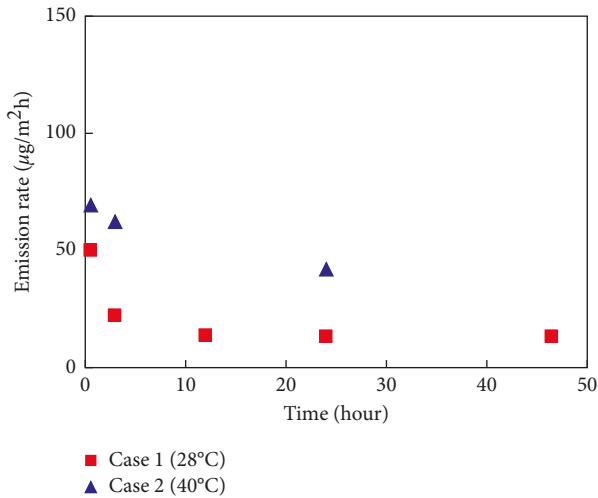
FIGURE 4: A plot of emission rate versus time showing the emission of di-2-ethylhexyl phthalate (DEHP) from the flooring specimen with regard to the temperature.
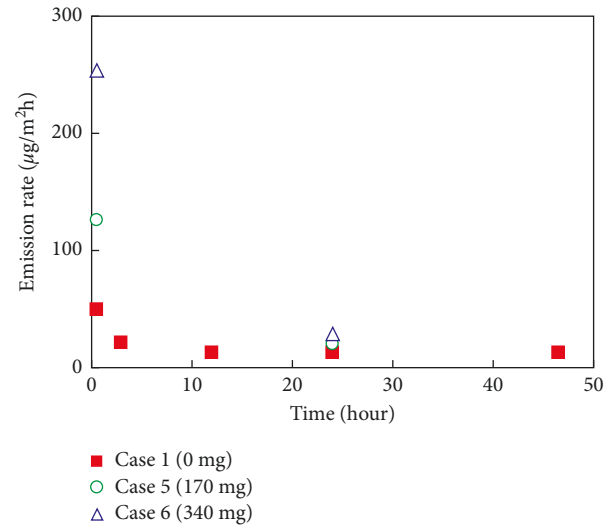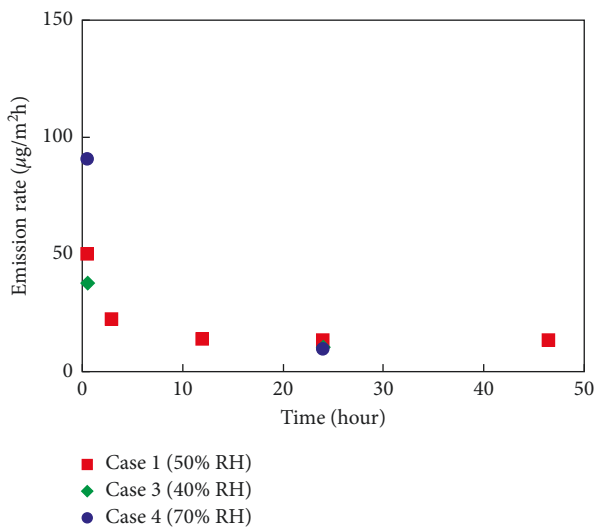

FIGURE 5: A plot of emission rate versus time showing the emission of DEHP from the flooring specimen with regard to relative humidity (RH).

experiment also confirms that a certain amount of time after the initiation of the experiment, the DEHP emission rate was not considerably influenced by the RH in the range 40%–70% (Figure 5).

3.3. Relation between DEHP Emission Rate and Airborne Particles. In case 5, quartz wool (170 mg) was placed in the microchamber as airborne particles. In case 6,340 mg of quartz wool was used. Table 6 and Figure 6 show the experimental results. In case 5, when 170 mg of quartz wool was placed in the microchamber, 2,733.0 ng of DEHP was collected and the DEHP emission rate was 20.6 μg/m^{2}h. Thus, the collected volume and emission rate were considerably greater than those in case 1 wherein no quartz wool was used

FIGURE 6: A plot of emission rate versus time showing the emission of DEHP from the flooring specimen with regard to airborne particles.

(amount of DEHP collected = 1,686.4 ng; DEHP emission rate = 20.6 μg/m^{2}h). In case 6 wherein 340 mg of quartz wool was used (amount of DEHP collected = 3,723.0 ng; DEHP emission rate = 29.1 μg/m^{2}h), the DEHP collection volume and emission rate were higher than those in case 5. This indicates that increasing the volume of airborne particles increases the area available for DEHP adsorption. It is thus believed that the SVOC emission rates are considerably affected by the adsorption surface area (the surface area of the interior of the microchamber and the surface area of the airborne particles).

3.4. Prediction Results for the Flow Field within the Microchamber. Table 7 and Figure 7 show the results of a CFD analysis of the airflow distribution, average air age, coefficient of the air change performance, and other factors for each case.

In case 7, the inlet speed of the microchamber supply was set to 2.1×10^{-2} m/s and the air exchange rate was set to 0.8 h^{-1}. In this case, the average airflow in the microchamber was 4.7×10^{-5} m/s and the airflow near the specimen was 3.5×10^{-5} m/s. In cases 8 and 9, the air exchange rate was set to 1.5 h^{-1}. In the experiments performed in these cases, the increase in the air exchange rate exhibited an increase in the average airflow in the microchamber (Table 7). In cases 7 (air exchange rate = 0.8 h^{-1}) and 8 (air exchange rate = 1.5 h^{-1}), the air flows straight up from the center of the microchamber, whereas in case 9 (air exchange rate = 4.0 h^{-1}), there is a large S-shaped airflow vector distribution. In cases 7 and 8, there is almost no circulating flow in the microchamber area as a whole. In contrast, in case 9, the high air supply rate causes the flow to collide with the front of the air inlet.

Figures 7(a)–7(c) show the air age [23] in the microchamber. These values are the average of local air ages at all points in the microchamber. Here, the local average air age is the amount of time required by air to move from the air inlet to an arbitrary point inside the microchamber.

TABLE 7: CFD analysis results (air exchange rate = 1.5 h^{-1}).

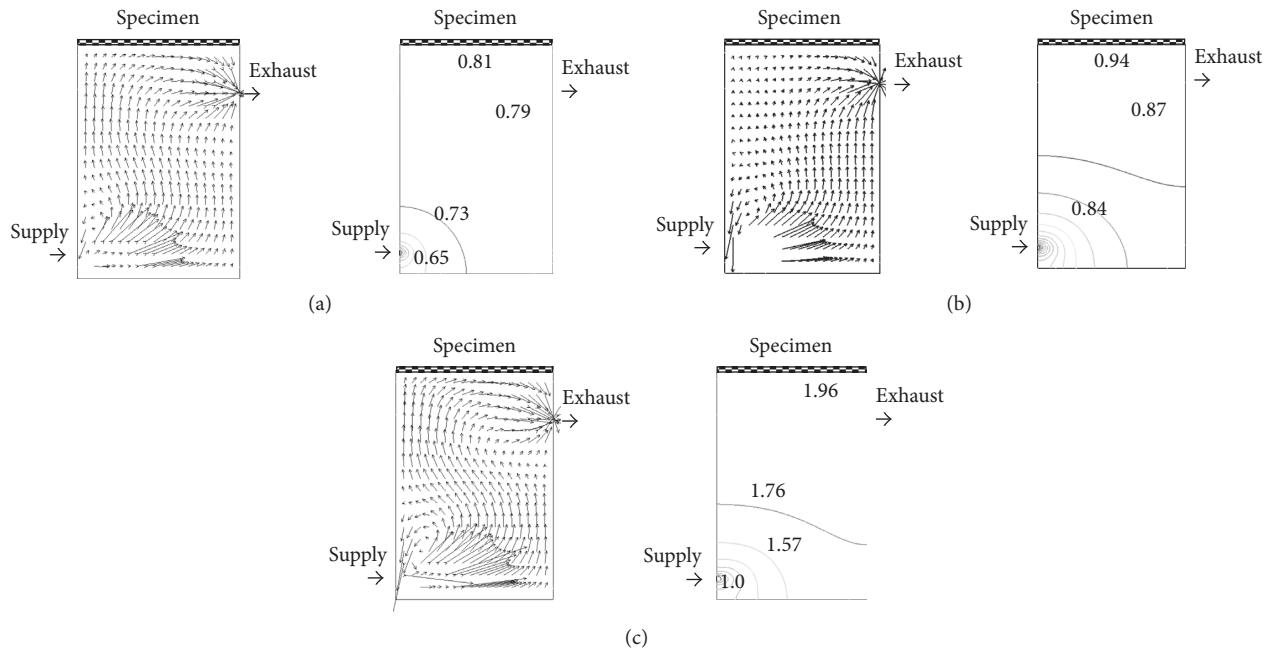| Case	7	8	9
Air exchange rate (h^{-1})	0.8	1.5	4.0
U_{in} (m/s)	2.1×10^{-2}	3.9×10^{-2}	5.2×10^{-2}
Average airflow in the microchamber (m/s)	4.7×10^{-5}	9.9×10^{-5}	1.5×10^{-4}
Airflow near the specimen (m/s)	3.5×10^{-5}	5.0×10^{-5}	5.0×10^{-5}
Mass transfer coefficient (m/h)	0.9	3.5	7.7
Average age of air in the microchamber	0.79	0.87	1.78
Coefficient of air change performance	1.6	0.8	0.1

FIGURE 7: Distribution of airflow vectors and air ages: (a) air change rate of 0.8 times/h, (b) air change rate of 1.5 times/h, and (c) air change rate of 4.0 times/h.

In cases 7–9, the average air age values in the microchamber were 0.79, 0.87, and 1.78, respectively. Thus, as the air exchange rate increased, the average air age tended to increase (Table 7). In particular, the air age values near the top of the microchamber (where the specimen was placed) were 0.81 in case 7, 0.94 in case 8, and 1.96 in case 9. Thus, fresh air required the maximum amount of time to travel from the microchamber's inlet to the top of the microchamber in case 9 wherein the air exchange rate was 4.0 h^{-1}. This may be because the high air supply rate in case 9 caused a circulating flow in the microchamber, as described above.

The coefficient of the air change performance corresponds to the air change performance in the microchamber. For example, if the air in the microchamber is in a completely mixed state, the coefficient of the air change performance will be 1 [23].

In case 7, the coefficient of the air change performance was 1.6. As shown in Figure 7(a), almost no stagnant areas or circulating flows were formed in the microchamber in this case. In case 8, the coefficient of the air change performance was 0.8. In this case, there was a slight stagnant area in the microchamber; however, the coefficient of the air change performance was close to 0.9, which is the stipulated

coefficient of the air change performance for a small chamber method in JIS A 1901 [23]. In case 9, the coefficient of the air change performance was 0.1. Thus, despite the high air exchange rate, there apparently was a high formation of stagnant areas and circulating flows in the microchamber (Figure 7(c)).

4. Discussion

As shown in Figures 4–6, the rate at which DEHP was emitted from the flooring specimen was high at the beginning of the experiments (0.5 h after the initiation of the experiment); however it gradually declined over time. 24 h after the initiation of the experiment, the emission rate stabilized. When experiments are conducted to measure SVOC emission rates using a microchamber, it is preferable to calculate the rates in the steady state that is reached 24 h after the initiation of the experiment.

Figure 8 shows a comparison of DEHP emission rates in the presence of factors influencing this rate. It was confirmed that the rate at which DEHP is emitted from the flooring specimen considerably depends on the temperature. An increase in the temperature excites the thermal motion of the
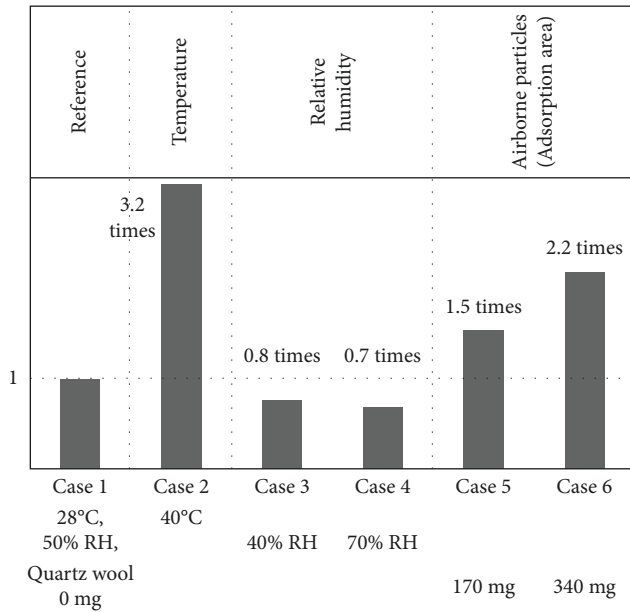
FIGURE 8: Comparison of DEHP emission rates in the presence of factors influencing this rate.

FIGURE 9: DEHP concentration distribution: air change rate = 1.5 times/h.

molecular chains, which has a significant impact on the emission of chemicals. The DEHP and resin chains contained in the flooring specimen are bound via intermolecular forces. The increases in temperature may gradually free the DEHP molecules from the resin, thereby increasing the DEHP emission rate. In contrast, there were no significant changes in the DEHP emission rates when the RH was changed. This may be because DEHP, which is hydrophobic, is not considerably influenced by humidity.

It was found that the increase in the adsorption area in the presence of airborne particles, that is, the increase in the surface area available for DEHP adsorption, is directly correlated to the increase in the DEHP emission rate. However, the increase in the DEHP emission rate was not directly proportional to the increase in the airborne particle volume because of the relation between the location of the emission source in the microchamber and the flow field. Figure 9 shows the results of an analysis performed under the conditions same as those in case 1 but with the surface concentration of the flooring specimen set to 298.3 $\mu g/m^3$. In this experiment, the DEHP emissions from the specimen were diffused; however, a concentration boundary layer was formed at the top of the microchamber wall. Additionally, the DEHP emissions were considerably influenced by the flow field (Figure 7(b)), possibly because DEHP is only adsorbed to a considerably small part of the microchamber walls at the top of the chamber (Figure 9). Although the extreme conditions must be considered (e.g., the walls' boundary conditions having unlimited adsorption capacity), DEHP was preferentially adsorbed to a part of the microchamber's interior surface that was near the emission source. Additionally, in cases wherein quartz wool was used as airborne particles, DEHP only adsorbed to a portion at the top of the quartz wool (in cases involving the use of 170 and 340 mg of quartz wool).
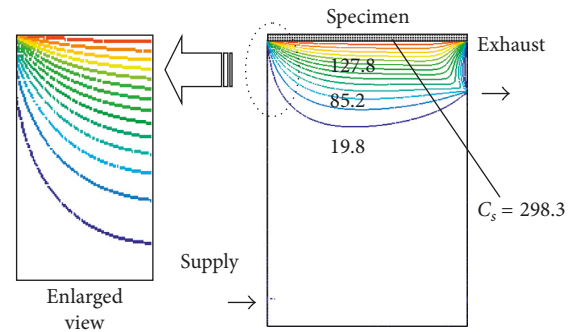
When the air exchange rate in the microchamber increased, the water vapor-equivalent mass transfer coefficient of the specimen surface rose. Despite this fact, stagnant areas and circulating flows also formed inside the microchamber, resulting in a far worse air change efficiency. Conversely, when a low air exchange rate was set, the air change efficiency in the microchamber was excellent; however, the mass transfer coefficient decreased to less than 1 m/h. The experimental findings suggest that supplying ventilation air (or helium) with an air exchange rate of ~1.5 h^{-1} is appropriate for the microchamber method.

5. Conclusions

Herein, we investigated the effects of temperature, RH, airborne particles, and air change properties on the emission rate of DEHP—an SVOC—using the microchamber method. Our results are summarized as follows:

(1) This research confirmed that the DEHP emission rate considerably depends on the temperature set for the experiment. When the microchamber method is utilized as the standard testing method, it is essential to set the temperature to a constant level to ensure that the performance of the experimental sample is evaluated uniformly.

(2) Although the DEHP emission rate was not shown to depend on humidity in this research, there is a need to investigate DEHP emission rates in low-humidity environments below 40% RH.

(3) Depending on the volume of airborne particles, we confirmed that placing quartz wool in the microchamber as airborne particles caused a considerable change in the DEHP emission rate.

(4) We set three patterns of air exchange rates and investigated the airflow characteristics in the microchamber for each pattern using the air change efficiency indicators of air age and coefficient of air change performance. With the microchamber method, it is preferable to conduct experiments with an air exchange rate of ~1.5 h^{-1}.

(5) It was shown that the emissions were greatly influenced by the flow field in the microchamber and

that nearly all SVOCs emitted by the specimen were only adsorbed to the inner walls at the top of the microchamber.

(6) The changes in the DEHP emission rates in low-temperature and low-humidity environments must be investigated. In the future, we plan to investigate the relation between emission rate and the factors influencing this rate for other types of SVOCs. We also plan to conduct experiments adapted to CFD analysis and verify the degree of adaptability to this type of analysis.

Conflicts of Interest

The authors declare that they have no conflicts of interest.

Acknowledgments

References

[1] C. G. Bornehag, J. Sundell, C. J. Weschler et al., "The association between asthma and allergic symptoms in children and phthalates in house dust: a nested case control study," *Environmental Health Perspectives*, vol. 112, no. 14, pp. 1393–1397, 2004.

[2] T. Salthammer and M. Wensing, "Flame retardants in the indoor environment part IV: classification of experimental data from house dust, indoor air and chamber tests," in *Proceedings of the 9th International Conference on Indoor Air Quality and Climate–Indoor Air 2002*, vol. 2, pp. 213–218, Monterey, CA, USA, July 2002.

[3] P. A. Clausen, V. Hansen, L. Gunnarsen, A. Afshari, and P. Wolkoff, "Emission of di-2-ethylhexyl phthalate from PVC flooring into air and uptake in dust: emission and sorption experiments in FLEC and CLIMPAQ," *Environmental Science & Technology*, vol. 38, no. 9, pp. 2531–2537, 2004.

[4] WHO, *Indoor Air Quality: Organic Pollutants, EURO Reports and Studies*, vol. 111, World Health Organization, Copenhagen, Denmark, 1987.

[5] J. J. Adibi, F. P. Perera, W. Jedrychowski et al., "Prenatal exposures to phthalates among women in New York City and Krakow, Poland," *Environmental Health Perspectives*, vol. 111, no. 14, pp. 1719–1722, 2003.

[6] C. J. Weschler, "Indoor/outdoor connections exemplified by processes that depend on an organic compound's saturation vapor pressure," *Atmospheric Environment*, vol. 37, no. 39-40, pp. 5455–5465, 2003.

[7] C. G. Bornehag, J. Sundell, and T. Sigsgaard, "Dampness in buildings and health (DBH): report from an on-going epidemiological investigation on the association between indoor environmental factors and health effects among children in Sweden," *Indoor Air*, vol. 14, no. 7, pp. 59–66, 2004.

[8] J. Pei, Y. Yin, J. Cao, Y. Sun, J. Liu, and Y. Zhang, "Time dependence of characteristic parameter for semi-volatile organic compounds (SVOCs) emitted from indoor materials," *Building and Environment*, vol. 125, no. 15, pp. 339–347, 2017.

[9] S. T. Larsen, R. M. Lund, G. D. Nielsen, P. Thygesen, and O. M. Poulsen, "Di-(2-ethylhexyl) phthalate possesses an adjuvant effect in a subcutaneous injection model with BALB/c mice," *Toxicology Letters*, vol. 125, no. 1–3, pp. 11–18, 2001.

[10] Y. Liang and Y. Xu, "The influence of surface sorption and air flow rate on phthalate emissions from vinyl flooring: measurement and modeling," *Atmospheric Environment*, vol. 103, pp. 147–155, 2015.

[11] M. Noguchi and A. Yamasaki, "Passive flux sampler measurements of emission rates of phthalates from poly(vinyl chloride) sheets," *Building and Environment*, vol. 100, pp. 197–202, 2016.

[12] Y. Sun, Q. Zhang, J. Hou, P. Wang, and J. Sundell, "Exposure of phthalates in residential buildings and its health effects," *Procedia Engineering*, vol. 205, pp. 1901–1904, 2017.

[13] P. A. Clausen, Y. Xu, V. Kofoed-Sørensen, J. C. Little, and P. Wolkoff, "The influence of humidity on the emission of di-(2-ethylhexyl) phthalate (DEHP) from vinyl flooring in the emission cell "FLEC"," *Atmospheric Environment*, vol. 41, no. 15, pp. 3217–3224, 2007.

[14] N.-Y. Hsu, Y.-C. Liu, C.-W. Lee, C.-C. Lee, and H.-J. Su, "Higher moisture content is associated with greater emissions of DEHP from PVC wallpaper," *Environmental Research*, vol. 152, pp. 1–6, 2017.

[15] T. Schripp, C. Fauck, and T. Salthammer, "Chamber studies on mass-transfer of di(2-ethylhexyl)phthalate (DEHP) and di-n-butylphthalate (DnBP) from emission sources into house dust," *Atmospheric Environment*, vol. 44, no. 24, pp. 2840–2845, 2010.

[16] H. Katsumata, S. Murakami, S. Kato, K. Hoshino, and Y. Ataka, "Measurement of semi-volatile organic compounds emitted from various types of indoor materials by thermal desorption test chamber method," *Building and Environment*, vol. 43, no. 3, pp. 378–383, 2008.

[17] Y.-F. Mao, Z. Li, Y.-L. He, and W.-Q. Tao, "CFD analysis of SVOC mass transfer in different chambers," *International Journal of Heat and Mass Transfer*, vol. 99, pp. 613–621, 2016.

[18] Y. Liang, O. Caillot, J. Zhang, J. Zhu, and Y. Xu, "Large-scale chamber investigation and simulation of phthalate emissions from vinyl flooring," *Building and Environment*, vol. 89, pp. 141–149, 2015.

[19] X. Liu, Z. Guo, and N. F. Roache, "Experimental method development for estimating solid-phase diffusion coefficients and material/air partition coefficients of SVOCs," *Atmospheric Environment*, vol. 89, pp. 76–84, 2014.

[20] Japanese Industrial Standards A 1904, *Determination of the Emission of Semi Volatile Organic Compounds for Building Products—Micro Chamber Method*, Japanese Standards Association, Tokyo, Japan, 2008.

[21] Y. Wu, S. S. Cox, Y. Xu et al., "A reference method for measuring emissions of SVOCs in small chambers," *Building and Environment*, vol. 95, pp. 126–132, 2016.

[22] Y. Li and J. Zhu, "Identification of sink spots in two thermal desorption GC/MS systems for the analysis of polycyclic aromatic hydrocarbons," *Analytica Chimica Acta*, vol. 961, pp. 67–73, 2017.

[23] Japanese Industrial Standards A 1901, *Determination of the Emission of Volatile Organic Compounds and Aldehydes for Building Products–Small Chamber Method*, Japanese Standards Association, Tokyo, Japan, 2003.

[24] *Ashrae Handbook, Fundamentals*, ASHRAE, Atlanta, GA, USA, 2017.

[25] K. Abe, T. Kondoh, and Y. Nagano, "A new turbulence model for predicting fluid flow and heat transfer in separating and reattaching flows—I. Flow field calculations," *International*

Journal of Heat and Mass Transfer, vol. 37, no. 1, pp. 139–151, 1994.

[26] Y. Ataka, S. Kato, S. Murakami, Q. Zhu, K. Ito, and T. Yokota, "Study of effect of adsorptive building material on formaldehyde concentrations: development of measuring methods and modeling of adsorption phenomena," *Indoor Air*, vol. 14, no. 8, pp. 51–64, 2004.

[27] The Society of Chemical Engineers, *The Handbook of the Chemical Engineering Science*, Maruzen Co., Ltd., Tokyo, Japan, 2001, in Japanese.